Article

Structural Evolution of Hexa-*peri*-hexabenzocoronene Adlayers in Heteroepitaxy on *n*-Pentacontane Template Monolayers

Luc Piot, Alexandr Marchenko, Jishan Wu, Klaus Mllen, and Denis Fichou

J. Am. Chem. Soc., **2005**, 127 (46), 16245-16250• DOI: 10.1021/ja0548844 • Publication Date (Web): 27 October 2005

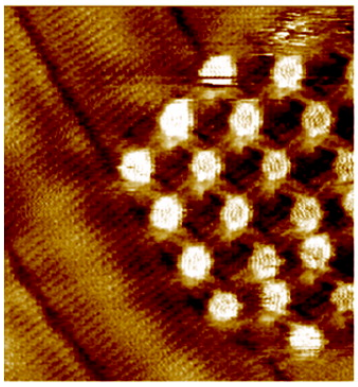

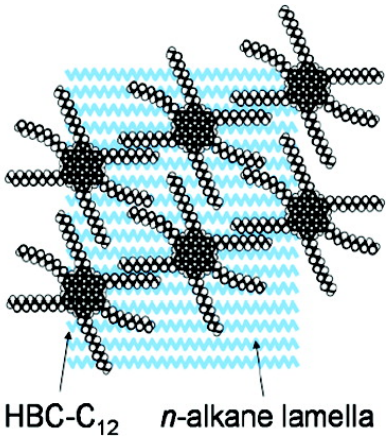

More About This Article

Additional resources and features associated with this article are available within the HTML version:

- Supporting Information
- Links to the 12 articles that cite this article, as of the time of this article download
- Access to high resolution figures
- Links to articles and content related to this article
- Copyright permission to reproduce figures and/or text from this article

View the Full Text HTML

J|A|C|S
ARTICLES
Published on Web 10/27/2005

Structural Evolution of Hexa-*peri*-hexabenzocoronene Adlayers in Heteroepitaxy on *n*-Pentacontane Template Monolayers

Luc Piot,[†] Alexandr Marchenko,[†] Jishan Wu,[‡] Klaus Müllen,[‡] and Denis Fichou*,[†]

Contribution from the CEA-Saclay, LRC Nanostructures et Semiconducteurs Organiques (CNRS-CEA-UPMC), SPCSI/DRECAM, 91191-Gif-sur-Yvette, France, Max-Planck-Institut für Polymer Research, Ackermannweg 10, 55128 Mainz, Germany

Received July 21, 2005; E-mail: fichou@drecam.cea.fr

Abstract: The growth and structure of self-assembled adlayers of hexakis(*n*-dodecyl)-*peri*-hexabenzocoronene (HBC-C_{12}) adsorbed on highly ordered pyrolitic graphite (HOPG) decorated by an *n*-pentacontane (*n*-$C_{50}H_{102}$) monolayer have been investigated by scanning tunneling microscopy (STM). Whereas on HOPG the HBC-C_{12} molecules readily self-assemble into a unique stable 2D structure, on the {*n*-$C_{50}H_{102}$ monolayer/graphite} system we observe morphological phase transitions with formation of time dependent α, β, and γ phases ($\alpha \rightarrow \beta \rightarrow \gamma$). The initial α-phase is similar to that obtained on bare graphite, while intermediate β- and final γ-structures present molecular dimers and rows, respectively. The observed two-dimensional polymorphism is due to weak interaction between HBC-C_{12} molecules and *n*-$C_{50}H_{102}$-modified graphite substrate. Our results constitute an important step toward the control of the growth and structure of highly ordered monolayers of functional conjugated molecules by modifying the graphite surface with an *n*-alkane monolayer of appropriate chain length.

1. Introduction

Disklike conjugated π-systems such as triphenylene, phthalocyanine, porphyrin, and hexa-*peri*-hexabenzocoronene (HBC) have recently emerged as a kind of important semiconductor with one-dimensional charge transport along the self-assembled columns.[1−4] Studies on their self-assembling properties have ranged from the bulk state to solution and to liquid−solid interfaces.[5−9] STM techniques disclosed 2D ordered monolayers at the solution/graphite or solution/Au(111) interfaces due to the strong interactions of these molecules with the substrates. Recently, composite organic layers (i.e., coadlayers having two or more organic components) have been presented as a further important step to achieve highly ordered organic nanostructures and also as an opportunity to fabricate molecular scale electronic devices on planar substrates.[10−19]

We propose here an approach for controlling the self-assembly process of a disklike graphite molecule, hexakis(*n*-dodecyl)-*peri*-hexabenzocoronene (HBC-C_{12}, Figure 1),[20] using an organic template formed by a long *n*-alkane (*n*-$C_{50}H_{102}$) deposited on highly ordered pyrolitic graphite (HOPG). It is well-known that long *n*-alkanes form stable closed packed lamellae-like structures on graphite. The stability and chemical inertness of *n*-alkanes films in ambient conditions allow one to consider them as a unique kind of substrate for heteroepitaxy of organic molecules. In the frame of this approach we demonstrate here that *n*-$C_{50}H_{102}$ highly ordered monolayers can be used as templates to induce new HBC-C_{12} packing. While the structures of monolayers of different HBCs have been already studied on graphite,[21] the real-time monitoring of structural changes at the molecular level has never been reported

[†] CEA-Saclay. CEA-Saclay also at UMR 7611 CNRS-UPMC, Université de Paris VI, 4 place Jussieu, 75005 Paris, France.
[‡] Max-Planck-Institut für Polymer Research.

(1) Adam, D.; Schumacher, P.; Simmerer, J.; Haussling, L.; Siemensmeyer, K.; Etzbach, K. H.; Ringsdorf, H.; Haarer, D. *Nature* **1994**, *371*, 141.
(2) Bushby, R. J.; Lozman, O. R. *Curr. Opin. Solid. State Mater. Sci.* **2002**, *6*, 569−578.
(3) Simpson, C. D.; Wu, J.; Watson, M. D.; Muellen, K. *J. Mater. Chem.* **2004**, *14*, 494−504.
(4) Wu, J.; Grimsdale, A. C.; Müllen, K. *J. Mater. Chem.* **2005**, *15*, 41−52.
(5) Samori, P.; Severin, N.; Simpson, C. D.; Müllen, K.; Rabe, J. P. *J. Am. Chem. Soc.* **2002**, *124*, 9454−9457.
(6) Saettel, N.; Katsonis, N.; Marchenko, A.; Teulade-Fichou, M.-P.; Fichou, D. *J. Mater. Chem.* **2005**, DOI: 10.1039/b504704h.
(7) Katsonis, N.; Marchenko, A.; Fichou, D. *J. Am. Chem. Soc.* **2002**, *124*, 9998−9999.
(8) Katsonis, N.; Marchenko, A.; Fichou, D. *J. Am. Chem. Soc.* **2003**, *125*, 13682−13683.
(9) Katsonis, N.; Marchenko, A.; Fichou, D. *Chem.−Eur. J.* **2003**, 9, 2574−2581.
(10) Jaeckel, F.; Watson, M. D.; Muellen, K.; Rabe, J. P. *Phys. Rev. Lett.* **2004**, *92*, 188303−1.
(11) Zeng, C.; Wang, B.; Li, B.; Hou, J. G. *Appl. Phys. Lett.* **2001**, *79*, 1685−1687.
(12) Lei, S. B.; Wang, C.; Yin, S. X.; Bai, C. L. *J. Phys. Chem. B* **2001**, *105*, 12272−12277.
(13) Lu, J.; Lei, S.; Zeng, Q.; Kang, S.; Wang, C.; Wan, L.; Bai, C. L. *J. Phys. Chem. B* **2004**, *108*, 5161−5165.
(14) Xu, S.; Yin, S.; Liang, H.; Wang, C.; Wan, L.; Bai, C. L. *J. Phys. Chem. B* **2003**, *108*, 6200−624.
(15) Lai, S.; Wang, C.; Fan, X.; Wan, L.; Bai, C. L. *Langmuir* **2003**, *19*, 9759−9763.
(16) Hoeppener, S.; Chi, L.; Fuchs, H. *Nano Lett.* **2002**, *2*, 459−463.
(17) Hickman, S.; Hamilton, A.; Patrick, D. L. *Surf. Sci.* **2003**, *537*, 113−122.
(18) Griessl, S.; Lackinger, M.; Edelwirth, M.; Hietschold, M. *Single Mol.* **2002**, *1*, 25−31.
(19) Sellam, F.; Schmitz-Huebsch, T.; Toerker, M.; Mannsfeld, S.; Proehl, H.; Fritz, T.; Leo, K.; Simpson, C. D.; Muellen, K. *Surf. Sci.* **2001**, *478*, 113−121.
(20) Stabel, A.; Herwig, P.; Müllen, K.; Rabe, J. P. *Angew. Chem., Int. Ed. Engl.* **1995**, *34*, 1609−1611.
(21) Samori, P.; Fechtenkötter, A.; Jackel F.; Böhme, T.; Müllen, K.; Rabe, J. P. *J. Am. Chem. Soc.* **2001**, *123*, 11462−11467.

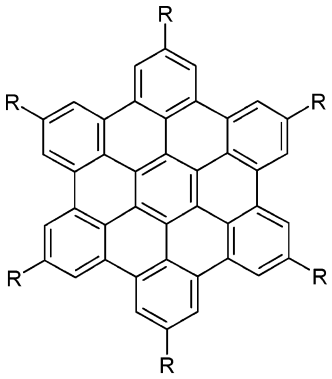

Figure 1. Chemical structure of HBC-C_{12}.

before. More generally, only a few studies report on the real space observation of the kinetics in a two-dimensional organic layer.[22−27] We show in this article that the HBC-C_{12} 2D-lattice undergoes two successive phase transitions induced by the presence of an *n*-alkane monolayer on top of the HOPG surface.

2. Experimental Section

Self-assembled monolayers of *n*-pentacontane (*n*-$C_{50}H_{102}$, >97%, Fluka) were deposited on freshly cleaved highly oriented pyrolitic graphite (HOPG) substrates (Goodfellow) from a solution (0.05 mg/mL) in *n*-tetradecane (*n*-$C_{14}H_{30}$, 99+%, Acros). The *n*-$C_{50}H_{102}$-modified HOPG samples were then rinsed with high-purity ethanol (99.9%, Merck) in order to remove the excess of *n*-$C_{50}H_{102}$. In a second step and after complete evaporation of ethanol, deposition of HBC-C_{12} was performed on the dry substrate using a saturated solution in *n*-tetradecane diluted 10 times. Room-temperature STM measurements were performed at the *n*-tetradecane/substrate interface in a constant current mode using a Pico-SPM (Molecular Imaging) equipped with a home-built liquid cell. A mechanically etched Pt/Ir (80:20) wire was used as the STM tip. Finally, it must be mentioned that several previous studies[9,28−30] have clearly shown that *n*-tetradecane molecules do not adsorb on HOPG under the experimental conditions used here.

3. Results

3.1. Structure of HBC-C_{12} on Bare Graphite. Although our main aim is to investigate self-assembly of an HBC-C_{12} overlayer deposited on *n*-$C_{50}H_{102}$-modified HOPG, we first performed STM observations of HBC-C_{12} deposited on bare HOPG. During the first 10 min after deposition, lateral growth of highly ordered monolayer islands extending over 100−200 nm takes place. HBC-C_{12} nucleates as submonolayer islands on flat terraces, whereas nucleation takes place neither at step edges nor at other morphological surface defects. From submonolayer coverage up to the monolayer, the ordered islands grow without changing their internal structure. Different concentrations are used without visible change in the structure of the monolayer and the growth regime.

Figure 2a shows a typical high-resolution STM image of an ordered HBC-C_{12} island. Each circular bright feature having a darker central part can be attributed to the π-conjugated cores of individual HBC-C_{12} molecules lying flat on the surface.[31] The linear features which are discernible between the cores are the dodecyl chains of HBC-C_{12}. As it can be seen in the enlarged STM image shown in the inset of Figure 2a, the alkyl chains form an angle of ~120° reflecting the symmetry of the underlying HOPG substrate. The crystallographic parameters of the two-dimensional HBC-C_{12} unit cell on graphite are $a = 3.5 \pm 0.05$ nm, $b = 3.2 \pm 0.05$ nm, and $\gamma = 87 \pm 1°$, and the average area per molecule is 5.6 ± 0.1 nm^2.

To check the long-term stability of these monolayers, we recorded a series of STM images in the same sample area over a period of 5−6 h. No significant evolution in either the location of the molecules or the 2D structure is observed. This implies that the HBC-C_{12} molecules are irreversibly physisorbed on the HOPG surface and that the surface mobility of individual molecules inside the islands is suppressed. Furthermore, a constant 2D structure is maintained when the tip bias is varied over a range of ±0.1−0.6 V, indicating that no field-induced phase transition takes place on bare graphite in this voltage range.

Surprisingly, we only observe one type of packing, whereas two different phases have been reported by Stabel et al.[20] This noticeable difference probably arises from the different tunneling liquids used in both experiments. Our STM measurements are performed in *n*-tetradecane, whereas these authors use 1,2,4-trichlorobenzene. In contrast to *n*-tetradecane which is nonpolar and chemically inert, 1,2,4-trichlorobenzene possesses a dipole moment, three (bulky) chlorine atoms, and a planar conjugated core. Therefore, interactions between HBC-C_{12} and 1,2,4-trichlorobenzene molecules are expected to take place and influence the packing arrangement.

3.2. Growth and Structure of HBC-C_{12} Adlayers on {*n*-$C_{50}H_{102}$ Monolayer/Graphite}. Similarly to shorter *n*-alkanes[32] *n*-$C_{50}H_{102}$ self-assembles readily on HOPG as large domains of parallel lamellae (see Figure 2b). Each lamella is constituted of molecules oriented perpendicular to the lamellae direction and parallel to the ⟨100⟩ direction of the HOPG lattice. The inset of Figure 2b is a submolecular resolution STM image which reveals the contribution of individual CH_2 groups of the *n*-$C_{50}H_{102}$ molecules.

Figure 3 shows two STM images of the {*n*-$C_{50}H_{102}$ monolayer/graphite} system partially covered by ordered domains of HBC-C_{12}. Nucleation takes place either along the step edges (Figure 3a) or in the middle of a terrace close to a morphological defect of the underlying *n*-$C_{50}H_{102}$ monolayer (Figure 3b). Both observations indicate that, in contrast to bare graphite, HBC-C_{12} molecules are mobile and diffuse on the *n*-$C_{50}H_{102}$ adlayer to self-assemble into ordered domains.

(22) De Feyter, S.; Larsson, M.; Schuurmans, N.; Verkuijl, B.; Zoriniants, G.; Gesquiere, A.; Abdel-Mottaleb, M. M.; van Esch, J.; Feringa, B. L.; van Stam, J.; De Schryver, F. *Chem.—Eur. J.* **2003**, *9* (5), 1198−1206.
(23) Gesquiere, A.; Abdel-Mottaleb, M. M.; De Feyter, S.; De Schryver, F. C.; Sieffert, M.; Mullen, K.; Calderone, A.; Lazzaroni, R.; Bredas, J. L. *Chem.—Eur. J.* **2000**, *6* (20), 3739−3746.
(24) Stabel, A.; Heinz, R.; Rabe, J. P.; Wegner, G.; Deschryver, F. C.; Corens, D.; Dehaen, W.; Siiling, C. *J. Phys. Chem.* **1995**, *99* (21), 8690−8697.
(25) Venkataraman, B.; Breen, J. J.; Flynn, G. W. *J. Phys. Chem.* **1995**, *99* (17), 6608−6619.
(26) Yang, Y. C.; Yen, Y. P.; Yang, L. Y. O.; Yau, S. L.; Itaya, K. *Langmuir* **2004**, *20* (23), 10030−10037.
(27) Vonau, F.; Suhr, D.; Aubel, D.; Bouteiller, L.; Reiter, G.; Simon, L. *Phys. Rev. Lett.* **2005**, *94* (6), 066103.
(28) McGonigal, G. C.; Bernhardt, R. H.; Thomson, D. J. *Appl. Phys. Lett.* **1990**, *57* (1), 28.
(29) Bucher, J. P.; Roeder, R.; Kern, K. *Surf. Sci.* **1993**, *289*, 370−380.
(30) Perronet, K.; Charra, F. *Surf. Sci.* **2004**, *551* (3), 213−218.
(31) Fisher, J.; Blochl, P. E. *Phys. Rev. Lett.* **1993**, *70*, 3263−3266.
(32) Wawkuschewski, A.; Cantow, H.; Magonov, S. N. *Langmuir* **1993**, *9*, 2778−2781.

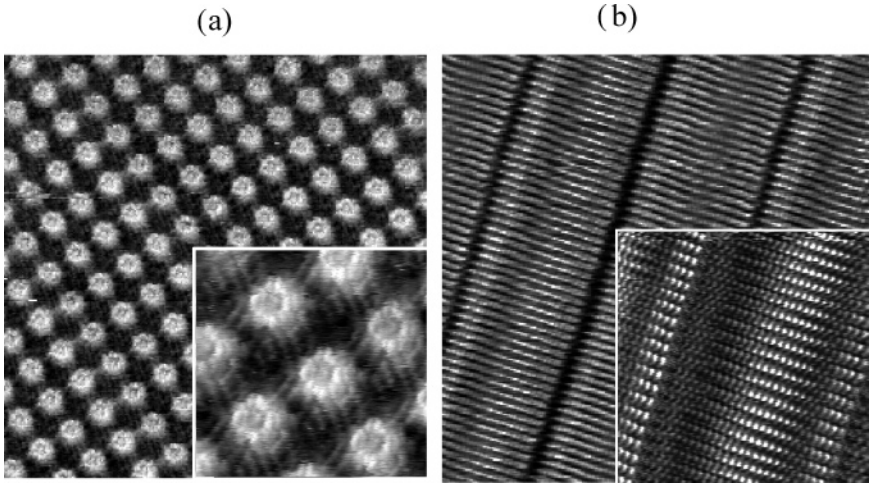

Figure 2. (a) STM constant current image of a self-assembled HBC-C_{12} monolayer physisorbed at the interface between *n*-tetradecane and graphite (18.7 × 18.7 nm^2; U_t = 670 mV, I_t = 16 pA). The inset shows intramolecular resolution of the HBC-C_{12} monolayer. The alignment of alkyl chains along crystallographic directions of graphite substrate is clearly visible (10.4 × 10.4 nm^2; U_t = −621 mV, I_t = 16 pA). (b) STM image (25 × 25 nm^2; U_t = −91 mV, I_t = 61 pA) of a self-assembled *n*-$C_{50}H_{102}$ monolayer adsorbed on graphite. The inset is a high-resolution STM image revealing individual CH_2 groups constitutive of each molecule (10 × 10 nm^2; U_t = −91 mV, I_t = 61 pA).

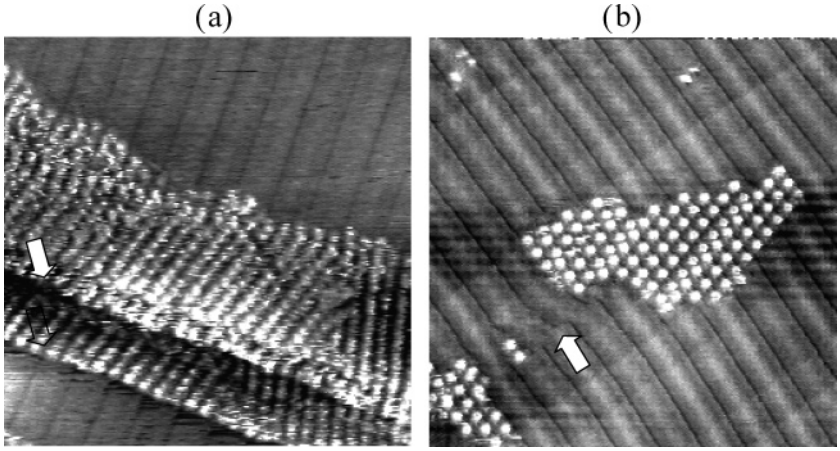

Figure 3. (a) STM image (81.8 × 81.8 nm^2; U_t = 152 mV, I_t = 9 pA) showing the step edges of templated graphite substrate (white arrows) decorated by close packed rows of HBC-C_{12} molecules (γ-phase). (b) The single island corresponding to the α-phase of HBC-C_{12} nucleated near misfit dislocation marked by white arrow (81.8 × 81.8 nm^2, U_t = 152 mV, I_t = 9 pA).

Within the time scale of our experiment (8 h), HBC-C_{12} self-assembles on the {*n*-$C_{50}H_{102}$ monolayer/graphite} system into three successive phases having, respectively, "oblique" (α-phase), "dimer" (β-phase), and "row" (γ-phase) configurations. These phases do not fit the HBC-C_{12} structure observed on bare graphite. We now describe the growth and structure of these three phases.

3.2.1. "Oblique Structure" (α-Phase). In the first 10 min following their deposition, the HBC-C_{12} molecules are not visible. However, in some areas the tunnel contrast of the *n*-$C_{50}H_{102}$ adlayer progressively becomes unclear, and ordered islands of HBC-C_{12} molecules appear. STM images show that the growth of the α-phase is completed and that no other phase coexists 1 h after deposition. Figure 4 shows two STM images recorded successively showing an HBC-C_{12} island (α-phase) and the characteristic lamellae structure of *n*-$C_{50}H_{102}$. To check that the HBC-C_{12} molecules are adsorbed on top of the *n*-$C_{50}H_{102}$ lamellae and not embedded into it, we lowered at the edge of one HBC-C_{12} domain the tunneling bias voltage to 100 mV and increased the tunneling current to 50 pA, expecting to induce a local perturbation of selected HBC-C_{12} molecules. Indeed, we observed that the molecules shown by white arrows in Figure 4a are desorbed to go back into *n*-tetradecane. As a result, at the very place of the desorbed HBC-C_{12} molecules the *n*-$C_{50}H_{102}$ lamellae become visible (Figure 4b). Tip-induced manipulation thus provides evidence that the HBC-C_{12} molecules are adsorbed directly on top of the *n*-C_{50} H_{102} adlayer instead of being embedded into it.

As it can be seen in Figure 4c, the aromatic cores of HBC-C_{12} molecules form an almost square packing, the parameters of the unit cell being $a = 3.5 \pm 0.05$ nm; $b = 3.2 \pm 0.05$ nm; $\gamma = 84 \pm 1°$. In this "oblique" packing arrangement, HBC-C_{12} rows are oriented at ∼15° in respect to the ⟨100⟩ direction of graphite while HBC-C_{12} columns are aligned strictly parallel to the ⟨210⟩ direction. Beside, two dodecyl chains per HBC-C_{12} molecule are aligned along the main axis of the *n*-$C_{50}H_{102}$ underlying ones, whereas two others form an angle close to 12° with the ⟨210⟩ direction of graphite. Finally, in this "oblique" α-phase the average area per molecule is $A_\alpha = 5.4 \pm 0.1$ nm^2, i.e., slightly smaller than that of HBC-C_{12} on bare graphite.

3.2.2. "Dimer Structure" (β-Phase). During the second hour after deposition of the HBC-C_{12} molecules, the initial α-phase evolves toward a "dimer structure" (noted β-phase), the α→β phase transition being completed within 2−3 h. A typical STM

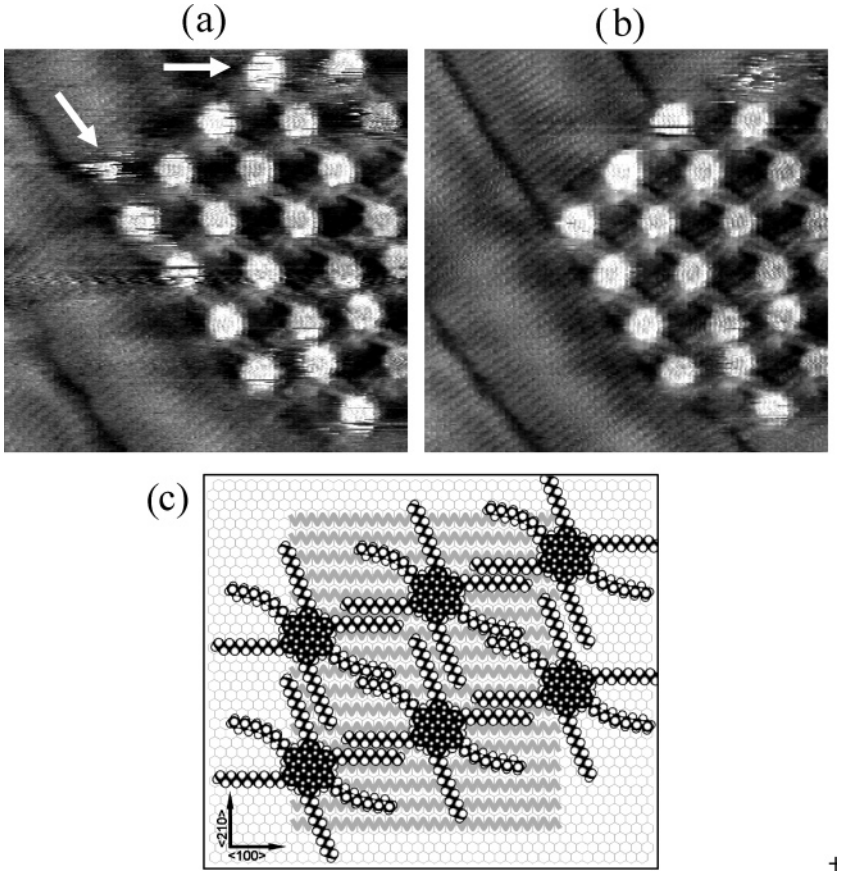

Figure 4. (a,b) Two consecutive STM images (18.7 × 18.7 nm^2, U_t = 634 mV, I_t = 5.4 pA) recorded 1 h after deposition of HBC-C_{12} with a time interval of 10 s. They show an HBC-C_{12} island having the α-phase adsorbed on top of the {*n*-$C_{50}H_{102}$ monolayer/graphite} system. The HBC-C_{12} molecules marked by white arrows are desorbed by the tip showing that the island is not embedded in the template but adsorbed on top of it. (c) Possible packing model of the α-phase. *n*-$C_{50}H_{102}$ molecules are depicted by gray zigzag lines on top of hexagonal graphite lattice.

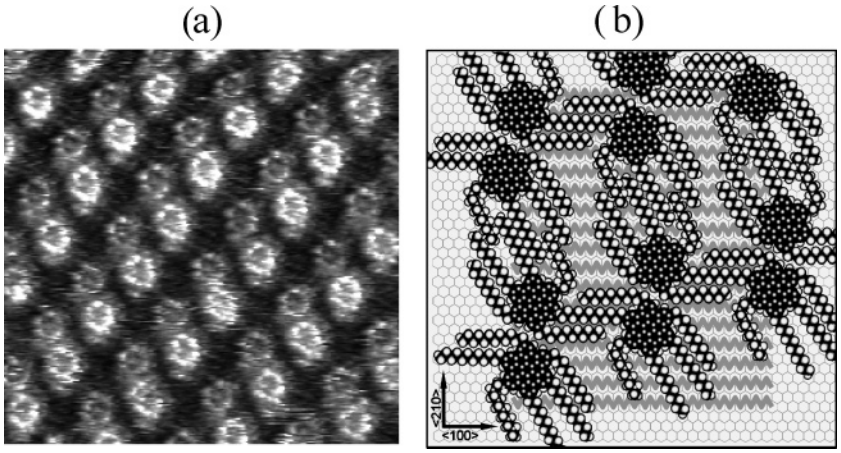

Figure 5. (a) STM image of β-phase (dimer structure) on top of the *n*-$C_{50}H_{102}$ monolayer. Two molecules within the dimer are not equivalent and have different STM contrast. Dodecyl chains of HBC-C_{12} occupy the space between the dimers and are aligned along preferential directions. (23.1 × 23.1 nm^2, U_t = 142 mV, I_t = 10 pA). (b) Possible packing model of the β-phase.

image of the β-phase is shown in Figure 5a. The aromatic cores of the HBC-C_{12} molecules within the dimers have different tunnel contrasts and are at a distance of ∼2.2 nm. The unit cell parameters are: $a = 5.6 \pm 0.05$ nm; $b = 3.6 \pm 0.05$ nm; $\gamma = 68 \pm 1°$. The average area per molecule is $A_\beta = 4.7 \pm 0.1$ nm^2, i.e., smaller than that for the α-phase ($A_\alpha = 5.4 \pm 0.1$ nm^2). In the β-phase, the dodecyl chains are interdigitated and aligned along the same directions as those in the α-phase. The separation distance between neighboring dodecyl chains (∼0.5 nm) is close to the equilibrium distance for bulk *n*-alkane values.[33] By taking into account all experimental distances as well as molecule dimensions and geometry, one possible packing model for the β-phase is presented in Figure 5b. The "dimer structure" in Figure 5a could have been interpreted as a double-tip artifact. However, Figure 6 reveals on the same STM image the coexistence of the β-phase together with the γ-phase (see below), thus ruling out such an interpretation.

(33) Fischbach, I.; Pakula, T.; Minkin, P.; Fechtenkötter, A.; Müllen, K.; Spiess, H. W.; Saalwächter, K. *J. Phys. Chem. B* **2002**, *106*, 6408−6418.

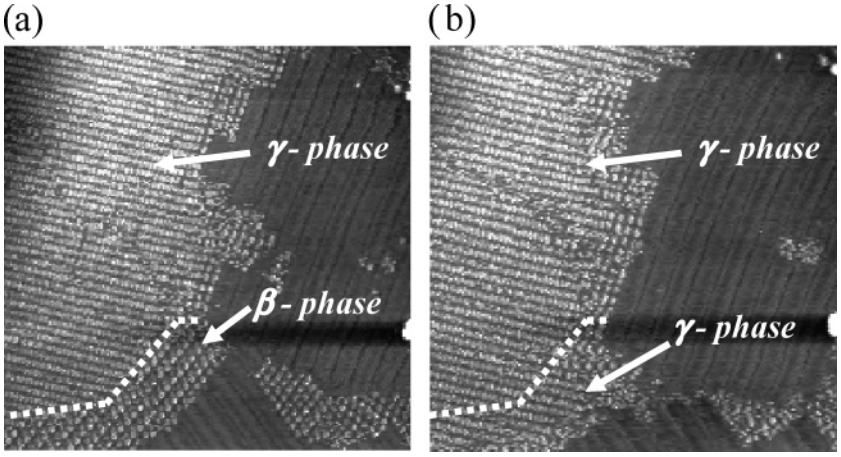

Figure 6. Consecutive STM images (198 × 198 nm^2; I_t = 10pA; U_t = 107 mV) recorded 5 h after deposition. The time interval between consecutive images is 4 min. (a) Coexisting intermediate β-phase and final γ-phase on top of *n*-$C_{50}H_{102}$ template. White dash line marks the boundary between two phases. (b) Propagation of γ-phase. The region in bottom part of the image is covered by γ-phase.

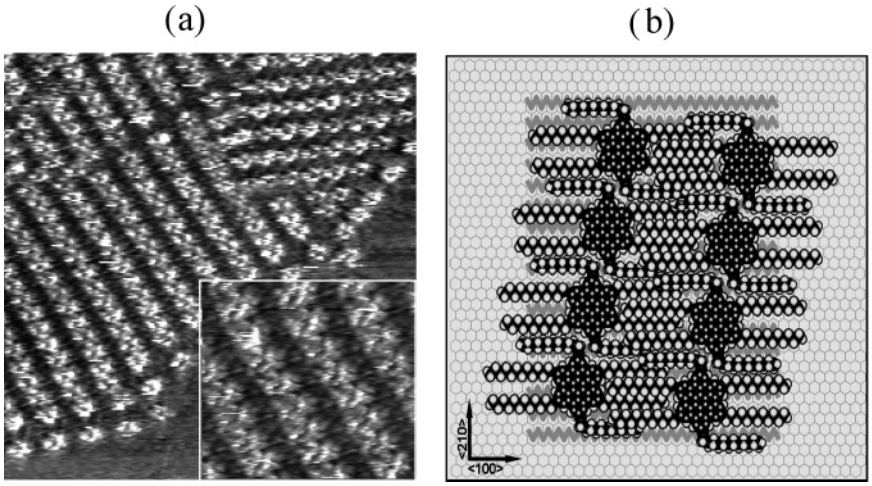

Figure 7. (a) STM image (37 × 37 nm^2, U_t = 584 mV, I_t = 6.4 pA) of the final γ-phase with a row structure. HBC-C_{12} cores form parallel rows on top of the *n*-$C_{50}H_{102}$ template. Inset shows details of packing (12 × 12 nm^2, U_t = 584mV, I_t = 6.4 pA). (b) Possible packing model of the γ-phase.

3.2.3. "Row Structure" (γ-Phase). A second transition takes place from the dimer structure into a final "row structure" (noted γ-phase) 5 to 6 h after HBC-C_{12} deposition. The two STM images of Figure 6 have been recorded within a 4 min period of time and illustrate the $\alpha \rightarrow \beta$ phase transition into a local domain. While Figure 6a clearly shows the coexistence of the β-phase (lower left) and γ-phase (upper left), Figure 6b shows that the β-phase has disappeared and has been transformed into a γ-phase domain. Finally, 6−8 h after deposition, the only visible phase is the γ-phase. We note that the coexistence of the initial α-phase and final γ-phase has never been observed during the experiment.

The high-resolution STM image in Figure 7a reveals the final "row structure" of HBC-C_{12} on the {*n*-$C_{50}H_{102}$ monolayer/graphite} system. A possible packing model is represented in Figure 7b. The molecular rows form an angle of ∼18° with the lamellae direction. Within a row, the distance between the centers of two consecutive aromatic cores is ∼2.0 nm, whereas two parallel rows are separated by ∼3.5 nm. We assume that the space between two rows is occupied by the dodecyl chains. The absence of clear STM features between the rows may be due to entanglement and flexibility of the alkyl chains. The unit cell parameters are $a = 2.0 \pm 0.05$ nm; $b = 3.5 \pm 0.05$ nm; $\gamma = 80 \pm 1°$. Note that average area per molecule, A_γ, for the γ-phase is the smallest ($A_\gamma = 3.2 \pm 0.1$ nm^2) against $A_\alpha = 4.7 \pm 0.1$ nm^2 and $A_\beta = 5.4 \pm 0.1$ nm^2.

Table 1. Lattice Parameters and Area Per HBC-C_{12} Molecules for Each Substrate and Phase

substrate	phase	lattice parameters	area per molecule (nm^2)
HOPG	rhombic	$a = 3.5 \pm 0.05$ nm $b = 3.2 \pm 0.05$ nm $\gamma = 87 \pm 1°$	5.6 ± 0.1
n-$C_{50}H_{102}$/HOPG	α-phase	$a = 3.2 \pm 0.05$ nm $b = 3.4 \pm 0.05$ nm $\gamma = 84 \pm 1°$	5.4 ± 0.1
n-$C_{50}H_{102}$/HOPG	β-phase	$a = 5.6 \pm 0.05$ nm $b = 3.6 \pm 0.05$ nm $\gamma = 68 \pm 1°$	4.7 ± 0.1
n-$C_{50}H_{102}$/HOPG	γ-phase	$a = 2.0 \pm 0.05$ nm $b = 3.5 \pm 0.05$ nm $\gamma = 80 \pm 1°$	3.2 ± 0.1

4. Discussion

Table 1 gathers the measured parameters of the unit cells for the various HBC-C_{12} phases observed on graphite and the {*n*-$C_{50}H_{102}$ monolayer/graphite} system. It reveals two remarkable features. First, the average area per molecule is maximized for the HBC-C_{12} self-assembly adsorbed directly on graphite (∼5.6

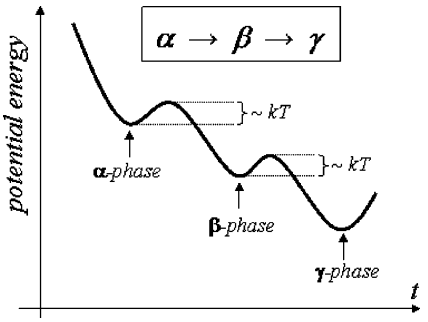

Figure 8. Scheme of the potential energy of the {HBC-C_{12}/*n*-$C_{50}H_{102}$/HOPG} system as a function of time. The heights of the α→*β* and *β*→*γ* energy barriers have to be close to the thermal activation energy level k_BT in order to enable the phase transitions.

nm^2). Second, this average area per molecule decreases from 5.4 nm^2 in the α-phase to 4.7 nm^2 in the *β*-phase to finally end up at 3.2 nm^2 in the *γ*-phase. This clearly demonstrates that the time evolution of the HBC-C_{12} 2D-structure on the {*n*-$C_{50}H_{102}$ monolayer/graphite} system is directed toward a higher density of packing.

In view of our results it seems that, while the α- and *β*-phases are metastable phases, the final stable *γ*-phase corresponds to the global minimum of potential energy in the {HBC-C_{12}/*n*-$C_{50}H_{102}$ monolayer/ graphite} system (Figure 8).

At this point, the question of the origin of such a structural transition arises, since under the same experimental conditions on a graphite surface no phase transition is observed. One can assume that the phase transition process is induced by two factors: first, the higher mobility of the HBC-C_{12} molecules on top of the *n*-$C_{50}H_{102}$ monolayer as compared to graphite; second, specific interactions between the HBC-C_{12} and *n*-$C_{50}H_{102}$ molecules leading to a template effect.

As mentioned above, in the presence of the *n*-$C_{50}H_{102}$ template, nucleation of the HBC-C_{12} molecules close to HOPG step edges or defects is observed, meaning that molecules are diffusing on atomically flat terraces (see Figure 3). In contrast, on bare graphite, nucleation also occurs on flat areas. This is an indirect evidence of the higher mobility of HBC-C_{12} molecules on the {*n*-$C_{50}H_{102}$ monolayer/graphite} surface as compared to bare graphite. This is not surprising since the interactions between the dodecyl chains of HBC-C_{12} are significantly stronger with HOPG than with the *n*-$C_{50}H_{102}$ molecules.[34] Since our experiments are performed at constant temperature (∼295 K) we assume that the diffusion barrier height of the HBC-C_{12} molecule on the {*n*-$C_{50}H_{102}$ monolayer/graphite} surface is close to the thermal activation energy at these conditions. The mobility conferred to the HBC-C_{12} molecules allows them to change in an easier way their location and configuration.

The *n*-$C_{50}H_{102}$ monolayer is acting as a template for the HBC-C_{12} overlayer, the lattice of which matches that of the underlying *n*-$C_{50}H_{102}$ for the three observed phases. From our results, it appears that the HBC-C_{12}/*n*-$C_{50}H_{102}$ interactions determine the packing mode of the HBC-C_{12} molecules essentially in two ways. They induce, first, an alignment of the HBC-C_{12} cores along the *n*-$C_{50}H_{102}$ lamellae direction (i.e., the ⟨100⟩ direction) and, second, an alignment of the dodecyl chains of HBC-C_{12} along the ⟨210⟩ direction due to self-recognition by the *n*-$C_{50}H_{102}$ molecules.

5. Conclusion

In summary, we present here a systematic investigation of the structural evolution of hexakis(*n*-dodecyl)-*peri*-hexabenzocoronene (HBC-C_{12}) on an *n*-$C_{50}H_{102}$ monolayer acting as a template. The growth of the physisorbed HBC-C_{12} molecules is slow enough to provide insight into their nucleation process and permits us to follow in detail the kinetics from the early stage of deposition over a time scale of several hours. In contrast to what happens on bare graphite, when the HBC-C_{12} molecules are adsorbed on an *n*-$C_{50}H_{102}$ template they self-assemble into three successive packing modes that can be summarized by the α→*β*→*γ* sequence of transitions. Therefore, deposition of large aromatic disklike molecules on HOPG modified by long *n*-alkane monolayers constitutes an original strategy for the fabrication of novel nanostructured surfaces. Our approach represents a particularly important step because it introduces two independent parameters that can be used for controlling the structure of a molecular 2D lattice. First the length of the *n*-alkane used as the template monolayer can be varied almost infinitely since ultralong monodisperse *n*-alkanes are available with chains containing up to 390 CH_2 units.[35−38] It is very likely that both the kinetics and the packing modes of a given planar molecule can be adjusted by fine-tuning of the *n*-alkane chain length. Second, the functional planar molecule in heteroepitaxy on the *n*-alkane/HOPG template can also be selected according to its further use. As a matter of fact, we are currently investigating various HBC derivatives as well as many other large graphitelike molecules in view of optimizing their 2D arrangement in view of their use in molecular devices.

JA0548844

(34) Sincotti, S.; Burda, J.; Hentschke, R.; Rabe, J. P. *Phys. Rev. E* **1995**, *51*, 2090.
(35) Hosier, I. L.; Bassett, D. C. *Polymer* **2002**, *43*, 5979−5984.
(36) Zeng, X.; Ungar, G. *Polymer* **2002**, *43*, 1657−1666.
(37) Zeng, X. B.; Ungar, G. *Macromolecules* **2001**, *34*, 6945−6954.
(38) Abo el Maaty, M. I.; Bassett, D. C. *Polymer* **2001**, 4965−4971.